# REPORT DOCUMENTATION PAGE

*Form Approved*
*OMB No. 0704-0188*



| 1. REPORT DATE *(DD-MM-YYYY)* | 2. REPORT TYPE | 3. DATES COVERED *(From - To)* |
|---|---|---|
| 30 April 2009 | Final | 1 October 2005 - 31 January 2009 |

**4. TITLE AND SUBTITLE**

Optical Forces in Polychromatic Light

**5a. CONTRACT NUMBER**

**5b. GRANT NUMBER**

N000140610038

**5c. PROGRAM ELEMENT NUMBER**

**6. AUTHOR(S)**

Harold Metealf

**5d. PROJECT NUMBER**

**5e. TASK NUMBER**

**5f. WORK UNIT NUMBER**

**7. PERFORMING ORGANIZATION NAME(S) AND ADDRESS(ES)**

The Research Foundation of S.U.N.Y.
Office of Sponsored Programs
Stony Brook, NY 11795-3362

**8. PERFORMING ORGANIZATION REPORT NUMBER**

NA

**9. SPONSORING/MONITORING AGENCY NAME(S) AND ADDRESS(ES)**

OFFICE OF NAVAL RESEARCH
800 NORTH QUINCY STREET
ARLINGTON VA 22217-5000

Charles Clark, Program Offieer

**10. SPONSOR/MONITOR'S ACRONYM(S)**

ONR

**11. SPONSOR/MONITOR'S REPORT NUMBER(S)**

**12. DISTRIBUTION/AVAILABILITY STATEMENT**

No restrictions

**13. SUPPLEMENTARY NOTES**

**14. ABSTRACT**

We work on optieal forees on atoms from non-monochromatic light. We have explored the bichromatic force, measured its properties, provided a dressed statc (Floquet) theory, and developed it into a practical tool for atomic nanofabrieation. In addition, we have explored frequeney swept light in adiabatic rapid passage to produce optical forces ten times larger than ordinary radiative forces. An extension of this theoretical description of the bichromatic force has led to some further understanding of the rolcs of spontaneous emission and entropy exchange in all forms of laser cooling. In addition, we have successed in produeing our first nanoscale structures. This is of special interest to the Navy because of its possible application for fabrication of multiply redundant atom chips, a feature necessary to help counteract the effects of decoherence. Several students have finished Ph.D.'s and Masters degrees and there havc been numerous papers and myriad abstraets for meetings.

**15. SUBJECT TERMS**

| 16. SECURITY CLASSIFICATION OF: | | | 17. LIMITATION OF ABSTRACT | 18. NUMBER OF PAGES | 19a. NAME OF RESPONSIBLE PERSON |
|---|---|---|---|---|---|
| a. REPORT | b. ABSTRACT | c. THIS PAGE | | | 19b. TELEPHONE NUMBER *(Include area code)* |
| | | | | | |

PROPOSAL SUBMITTED TO:
OFFICE OF NAVAL RESEARCH
800 NORTH QUINCY STREET
ARLINGTON VA 22217-5000

by
The Research Foundation of S.U.N.Y.
Office of Sponsored Programs
Stony Brook, NY 11795-3362

A Private, Non-Profit Organization and FDP Participant

# COOLING AND TRAPPING OF NEUTRAL ATOMS

Submitted Pursuant to ONR BAA08-001

Cognizant Program Officer:

**Dr. Charles Clark, Electronics (Code 312)**

A Three Year Project Costing a Total of $ 429,607
Project Start Date is 3 July 2005

**Prof. Harold Metcalf**
Physics and Astronomy Dept.
State University of New York
Stony Brook, NY 11794-3800

Phone: (631)632-8185 (voice) (631)632-8176 (FAX)
Email: hmetcalf@notes.cc.sunysb.edu

Authorizing Institutional Official's Signature: Lydia Chabza

Name: **Lydia Chabza** Title: **Sponsored Programs Coordinator**

Phone: (631)632-4849 (voice) (631)632-6963 (FAX)

# I. OVERVIEW

This document is a final report on grant # N000140610038 (local number 37982) entitled "Cooling and Trapping of Neutral Atoms" to Harold Metcalf and his colleagues that terminated 30 September 2008.

Since our work on optical forces on atoms from non-monochromatic light began, we have explored the bichromatic force, measured its properties, provided a dressed state (Floquet) theory, and developed it into a practical tool for atomic nanofabrication. In addition, we have explored frequency swept light in adiabatic rapid passage to produce optical forces ten times larger than ordinary radiative forces (see Section II A 2). An extension of this theoretical description of the bichromatic force has led to some further understanding of the roles of spontaneous emission and entropy exchange in all forms of laser cooling (Section II B). In Section II C we describe our successes in producing our first nanoscale structures. This is of special interest to the Navy because of its possible application for fabrication of multiply redundant atom chips, a feature necessary to help counteract the effects of decoherence. Several students have finished Ph.D.'s and Masters degrees and there have been numerous papers and myriad abstracts for meetings (Section II D).

# II. ACCOMPLISHMENTS SUPPORTED BY THE GRANT

## A. Optical Forces in Polychromatic Light

### 1. *Introduction*

Early laser cooling experiments were understood in terms of two-level atoms moving in a monochromatic light field [1]. This simple view could describe beam deceleration, dipole force traps, optical molasses, and lattices and band structure effects. Later the extension from two-level to multi-level atoms opened up entirely new areas of study and provided a whole new set of tools. One might anticipate a similar plethora of new phenomena to arise from the application of non-monochromatic light, such as different frequencies or changing frequencies, but this topic has has not received as much attention. The first such experiments were reported in Ref. [2], and since then we have been studying optical forces in such non-monochromatic light [3–14].

With the usual radiative force from monochromatic light that has been exploited for laser cooling for the past 25 years, the momentum exchange proceeds by absorption followed by spontaneous emission, and it saturates at a maximum value of $F_{rad} \equiv \hbar k\gamma/2$. Moreover, the natural width imposes a velocity range for the force, limited to $\pm\gamma/k$. In sub-Doppler cooling of multilevel atoms, it is the dipole force that works on the atoms. Even though the dipole force does not saturate, its velocity-dependent damping part is limited by $\gamma$. Also, the optical pumping rate $\gamma_p < \gamma$ imposes a velocity range $\pm\gamma_p/k$. Our measurements have shown that polychromatic light doesn't simply overcome these limits of force magnitude and velocity range, but exceeds them by an order of magnitude or more. In fact, the limit may be imposed only by laser and modulator technology.

### 2. *Studies of Adiabatic Rapid Passage*

The original proposal for the expiring grant described our plans for exploring and demonstrating extremely large optical forces using adiabatic rapid passage (ARP), a long-studied method of inverting the population of a two-level system that was well known since the early days of magnetic resonance. Now this has been accomplished and the results have been presented in Ref's. [5, 15]. We reported measured forces much larger than the radiative force that corresponded well with these calculations, but still not as large as predicted by our model.

Exploitation of ARP for producing large optical forces requires repeated frequency sweeps with differently directed light beams that coherently exchange momentum between them, imparting the difference to the atoms. The most common case is counterpropagating beams where $2\hbar k$ is exchanged in each cycle. The idea to investigate ARP grew out of the notions of coherent control of momentum transfer between light and atoms. Since the momentum exchange per cycle $2\hbar k \ll$ typical atomic momentum, this has to be repeated $\sim 10^4$ times in order to have a significant effect. It is clear that ARP can be effective when atoms redirect light from one beam into another, and so the idea of using ARP to cause absorption of light from one beam and stimulated emission into another came to mind.

Perhaps the easiest way to envision the ARP process is in a dressed atom view of the energies of a two-level system. The energies of a pair of coupled levels in this picture are $E_\pm = \pm(\hbar/2)\sqrt{\delta^2 + \Omega^2}$ where $\delta \equiv \omega_\ell - \omega_a$ is the detuning of the light at frequency $\omega_\ell$ from atomic resonance at $\omega_a$, and $\Omega \equiv e\langle g|\vec{\mathcal{E}} \cdot \vec{r}|e\rangle/\hbar$ is the Rabi frequency that characterizes the on-resonance, electric dipole interaction between the light and atoms.

An important aspect of the dressed atom picture for the present concern is the energy ordering of the eigenstates. In the low-intensity domain (characterized by $\Omega < \delta$) the upper eigenstate approaches the ground state $|g\rangle$ and the lower one approaches the excited state $|e\rangle$ for the case of $\delta > 0$ but the reverse is true for $\delta < 0$. A plot of $E_\pm$ is shown in Fig. 1 showing these limits near the $\Omega = 0$ plane. These bare ground and excited states $|g\rangle$ and $|e\rangle$ are otherwise mixed on two eigenenergy sheets away from the low intensity limit (see Ref. [16]).

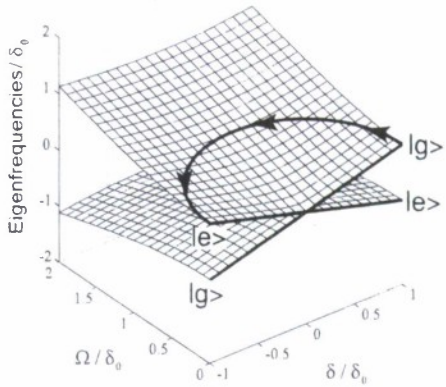


FIG. 1: A plot of $E_\pm$. The dressed states comprise two separated sheets except at the conical intersection at the origin. The upper (lower) state is ground at $\Omega = 0$ for $\delta > 0$ ($\delta < 0$). The indicated path is a possible trajectory for ARP.

The process of ARP in this view involves a synchronized sweep (fast enough to avoid deleterious effects from spontaneous emission) of both the amplitude and frequency of the light so that the state of the system follows a trajectory similar to that of the heavy line in Fig. 1 ($\delta_0$ is the amplitude of the frequency sweep). As long as travel along this trajectory is slow enough to avoid a non-adiabatic transition to the complementary eigenenergy sheet, the population will be completely inverted. Travel on the lower energy sheet can be similarly adiabatic. The special case of $\Omega_{\max} = \delta_0$ was solved analytically in Ref. [17].

Production of a strong optical force on atoms would require very many such repetitive sweeps that each exchange momentum $\hbar k$, and so the probability for non-adiabatic transitions must be kept very small for this to be successful. The probability of such unwanted transitions can be found from the small fraction of population on the "wrong" energy sheet at the end of each sweep where $\Omega = 0$ so the eigenstates are exactly the bare states.

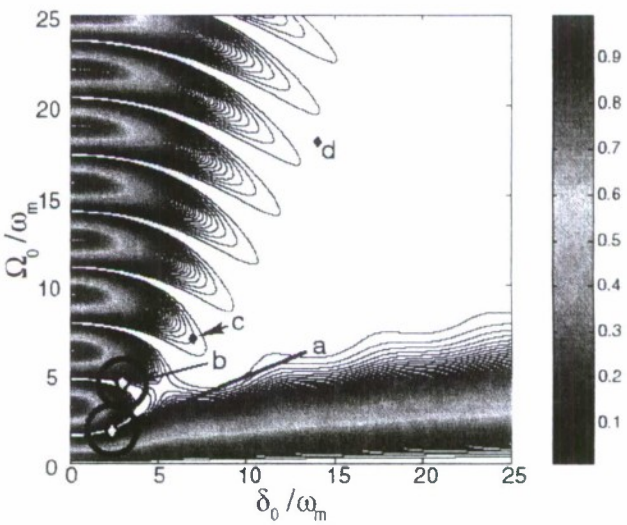


FIG. 2: A contour plot of the numerical values of the residual ground state population $\rho_{gg}$ vs. $\delta_0$ and $\Omega_0$ after one sweep (this is best viewed in color). The large open areas toward the upper right represent regions where $\rho_{gg} < .01$ so the probability of non-adiabatic transitions is negligibly small. Interest lies in those special areas that are close to the origin where $\rho_{gg}$ is still tiny. The pathway along the vertical axis, $\delta_0 = 0$, that is punctuated by narrow white regions represents pulses of area $n\pi$ that also produce inversion ($n$ = odd integer). The indicated points represent $(\delta_0/\omega_m, \Omega_0/\omega_m)$ = (a) - (2.4, 1.8), (b) - (3, 4.4), (c) - (7, 7), and (d) - (14, 18). (Figure from Ref. [3].)

In Ref. [3] we calculated the conditions that optimized this momentum transfer in the parameter space of $\delta_0$ and $\Omega$, by integrating the equation of motion of the Bloch vector on the Bloch sphere. We very quickly discovered unexpected behavior of nearly closed orbits and in Ref. [4] we provided an expansion of those views to non-ideal sweeps. Figure 2 shows a contour plot of the of the regions of parameter space that minimize the residual ground state population after a single sweep. The usual viewpoint is that the ARP mechanism works in the large open areas of the upper right quadrant, but there are clearly other regions where it will also work well.

We chose to do experiments in the region near point (a) of Fig. 2 because it seemed like the most unusual place for ARP to be effective, and because it was the easiest to reach experimentally. Our successes are described in Ref's. [5, 15] and are summarized in Fig. 3. However, we found that the overall magnitude of the force was less than half of the value predicted by our simple model.

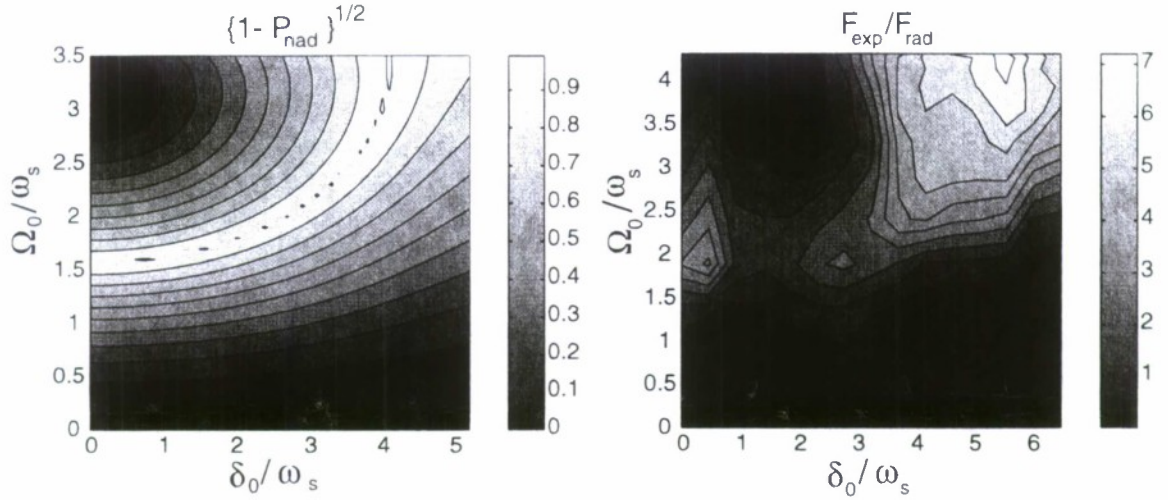


FIG. 3: Part (a) shows a calculated map of the nonadiabatic transition probability of Ref. [3] from which the force can be calculated directly, and part (b) shows the force we extracted from our measurements. Lighter areas correspond to larger forces. The qualitative agreement is quite excellent. (Fig. from Ref. [5].)

In Ref. [5] we suggested that the problem may be incomplete optical pumping to the $J = 1$, $M_J = +1$ sublevel required to make this a true two-level atom in a cycling transition. Although the maximum possible pumping rate is $\gamma/2$, our detuning is sufficiently large that the excitation rate is considerably smaller. Thus the characteristic time for even the first step in the optical pumping process is $30\,\tau$ corresponding to travel through nearly 1/3 of the interaction region. More careful modelling of these processes suggests that half of the atoms are lost, a result consistent with our measurements.

We therefore designed and built magnet coils and installed an adequate pre-pumping region upstream of the ARP region. The result was a substantial increase of the measured force and a paper is in preparation [6], but the magnitude of the force still remains well below that of our model. Not only that, but we found that the optical pumping light beam made little improvement once the magnetic environment was controlled.

### *3. An Interesting Bichromatic Field Result*

Many of the features of the bichromatic force had already been explored when the original proposal was written, and were presented there as recent accomplishments. Almost all of our experimental work in this area has previously been published in various articles [7–14] so the topic won't be discussed here. However, we have found a number of curious results from our new calculations that began in the summer of 2007. One of these is the behavior of the eigenfunctions of two-level atoms in a two-frequency field. Our calculations first reproduced the eigenvalues of the Floquet Hamiltonian given in Ref. [11] and then examined the eigenvectors belonging to them.

Over a very wide range of parameters, we have found that these eigenvectors conform with our intuition in some cases, but to give eye-opening results in others. For the former, we note that the expansion coefficients have the expected spatial symmetry and appropriately vanish at the nodes of the fields that connect them to other states. For the latter, we were surprised to see that the eigenstates of bichromatic light allow an average inverted population of a two-level atom in steady state, a situation forbidden in monochromatic light. This surprising result has now been described with a simple intuitive model on the Bloch sphere as well as formal solution of the Schrödinger equation in which the absence of the rotating wave approximation accounts for the two frequencies [18].

This result can be described in terms of the motion of the Bloch vector $\vec{R}$ on the Bloch sphere given by $d\vec{R}/dt = \vec{\Omega} \times \vec{R}$, where $\vec{\Omega}$ is the usual artificial 3-vector $(\Omega, 0, \delta)$, $\Omega$ is the Rabi frequency of the atom-light transition for light of frequency $\omega_\ell$ detuned from the atomic frequency $\omega_a$ by $\delta \equiv \omega_\ell - \omega_a$. In such single-frequency light the eigenstates (stationary states) are necessarily those having $\vec{R} \parallel \pm\vec{\Omega}$ so that $d\vec{R}/dt = 0$.

These two dressed eigenstates of the atom-field system reside on the upper and lower hemispheres of the Bloch sphere, and can only approach the equator in the limit $\delta/\Omega \to 0$, but cannot cross it.

Quite the reverse is true in a bichromatic field. The infinite Floquet Hamiltonian is tri-diagonal as given in Ref. [11] and the spatial dependence of its eigenvalues is plotted there. However, the eigenvectors were not studied until this past summer (2007) when a student plotted their dependence on $\Omega$.

She found that in the limit of $\Omega/\delta \to 0$ the eigenstates are the ground and excited states as expected, but they become strongly mixed near $\Omega/\delta \sim 1$, so we call them $|1\rangle$ and $|2\rangle$ in analogy to the usual dressed state labelling. In this region, the alternate Floquet states have the same mixtures of ground and excited state components, again as expected. However, unlike the case for monochromatic light discussed above, her surprising results in the bichromatic field show that these states can switch identities so that a primarily ground state at low values of $\Omega/\delta$ can be primarily excited near $\Omega/\delta \approx 2$ (see Fig. 4). These states have stable maxima in this opposite sense near $\Omega/\delta \approx 2.8$.

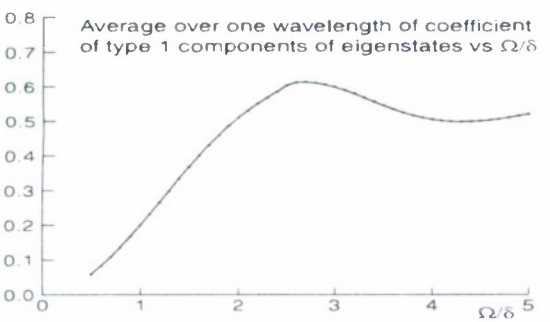


FIG. 4: The spatially averaged excited state component of type $|1\rangle$ eigenstates *vs.* $\Omega/\delta$. Near zero it is mostly ground state, but becomes strongly mixed near $\Omega/\delta \sim 1$. What is surprising is the region above 2 where more than 50% of its composition is excited state, which means it spends most of its time on the upper hemisphere of the Bloch sphere.

The model that helps us to describe this is based on the beat frequency pattern of the bichromatic field as shown in Fig. 5. We imagine it to be a single frequency so that the Bloch sphere picture is suitable, but its amplitude is modulated. When the two frequencies are equally spaced above and below atomic resonance, the carrier frequency is resonant so $\vec{\Omega}$ lies on the equator, and its large amplitude at short times drives $\vec{R}$ away from the south pole very rapidly. $\vec{R}$ reaches the equator in a short time, but by then the amplitude of the driving field (still precisely resonant) has begun to decrease. Thus the traversal of $\vec{R}$ across the upper hemisphere is much slower, and in fact, is a minimum if it passes the north pole just where the amplitude vanishes in Fig. 5 (*i.e.*, one-half the pattern shown is a $\pi$-pulse.) Then $\vec{R}$ spends much more of its total time in the upper hemisphere even though it is primarily a "ground" state.

FIG. 5: The beat pattern of two closely-spaced frequencies as appropriate for the bichromatic field. It the early part of the beat cycle the amplitude is quite large and the Bloch vector $\vec{R}$ precesses rapidly about $\vec{\Omega}$ reaching the equator in a short time. However, its traversal of the upper hemisphere is much slower because of the smaller amplitude, so its dwell time there is much longer.

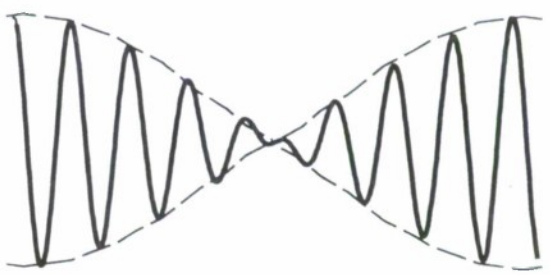

### B. Studies of Entropy Exchange in Laser Cooling

#### *1. Introduction*

Laser cooling is typically described in terms of optical forces from monochromatic light whose velocity dependence reduces the width of the velocity distribution of an ensemble of atoms. Because there are very many different phenomena involved, considerable care is necessary to keep their descriptions separate from one another and not mix up the intuitive notions from each of these various effects. For example, it is a long-standing and widely held tenet in the laser cooling community that spontaneous emission is required to carry away the entropy lost by a vapor of atoms being cooled. But this is often misconstrued to mean that spontaneous emission is always required for laser cooling. We showed how cooling could occur without it, and proposed an experimental test of this completely unexpected possibility.

We begin by showing that spontaneous emission is not the only way of removing the entropy, and that the laser fields themselves are capable of absorbing it [26]. This is because spontaneous emission does this by redistributing the light among a multitude of accessible states in the Hilbert space, and stimulated emission can do precisely the same thing. Our calculation compares the entropy lost by the cooled atoms with the entropy capacity of the laser fields. The description requires that the light field be included as part of the system, and not just as an externally applied potential.

In the usual $(\Delta E, \Delta p)$ description of laser cooling, the force is calculated from the momentum of absorbed light $h\nu/c \equiv \hbar k$ or $\mathrm{tr}(\rho \nabla \mathcal{H})$. Then the kinetic energy exchange between atoms and light involves Doppler shifts or spatially-dependent light shifts in inhomogeneous optical fields. The velocity-dependent force moves all the atoms in an extended region of velocity space to a narrower region so the velocity distribution is compressed. In these usual $(\Delta E, \Delta p)$ views, the laser light is treated as a classical field with a fixed potential, and the entropy loss is usually dismissed with vague references to spontaneous emission, without any proof.

When light is absorbed by an atom, its internal energy increase is compensated by an energy decrease of the light field. A popular way to depict this energy conservation process is the Jaynes-Cummings view, where the light field can be described as a number state. Then it becomes clear that some energy from the light field is transferred to the atom, but only if the light field is part of the system.

### 2. *A Closer Look at Doppler Cooling*

As an example, consider the case of Doppler cooling where the $(\Delta E, \Delta p)$ description is incomplete because its velocity-dependent damping force does not conserve energy. The velocity dependence arises because the resonance condition, and hence the optical force, depends on the Doppler shift seen by moving atoms, $\omega_D \equiv -\vec{k} \cdot \vec{v}$,. That is, the absorbed light frequency is $\omega_\ell = \omega_a - \omega_D$, where $\omega_a$ is the atomic frequency whereas the average emitted light frequency is $\omega_a > \omega_\ell$. The kinetic energy change on absorption is $\Delta \mathrm{KE} = mv\Delta v = \hbar k v = -\hbar\omega_D$ (for $v \gg \Delta v = \hbar k/M$). Then energy conservation is satisfied with a velocity-dependent force when the light field is included in the system because there is simply an energy exchange between the atoms and the light through the Doppler shift $\omega_D$. Analogous arguments apply to the velocity dependence of other cases of $(\Delta E, \Delta p)$ exchanges.

The most naive $(\Delta E, \Delta p)$ view of laser cooling violates the unitarity theorem. That is, atoms with initially different velocities have initially orthogonal wave functions because of their different deBroglie wavelengths. After cooling, their deBroglie wavelengths may be sufficiently similar that their wave packets are no longer orthogonal, thereby violating the theorem. Unitarity in Doppler cooling may be rescued by including the spontaneously emitted light from the excited atoms into the system because the fluorescence generally occupies orthogonal states of the radiation field thereby preserving the theorem. In the discussion below, we show that changes to the laser field itself are sufficient to preserve unitarity.

In this review of Doppler cooling, we have seen that including the optical field provides for satisfying three conditions: 1) energy conservation between the atomic internal energy and the field, 2) energy conservation between the atomic motion and the field, and 3) preservation of unitarity. Similar arguments hold for other laser cooling schemes.

### 3. *Phase Space Considerations*

We now extend the discussion beyond the limits of the usual $(\Delta E, \Delta p)$ view and treat the laser field as a dynamical variable. This notion is substantiated in the very eloquent statement from Ref . [27]:

> "What do we do next? ... Begin by deciding how much of the universe needs to be brought into the discussion. Decide what normal modes are needed for an adequate treatment of the problem under consideration. Find a suitable approximation for the normal modes; the simpler, the better. Decide how to model the light sources and work out how they drive the wave function for the system."

Although this seems a bit superficial at first, in fact it's very profound. A complete description of the dynamics of any of these laser cooling processes requires that the entire light field be considered as part of the system. Only then can it absorb entropy and transport it out of the system. Spontaneous emission simply redistributes the light into some subset of a much larger set of accessible states, and stimulated emission can do likewise. Thus the exchange of entropy between the atoms and the light field does not violate the Liouville theorem, unitarity, or Ref. [28] because neither the total entropy of the system nor its phase space volume is reduced, but merely exchanged between its different parts.

Our 1-D comparison with the entropy capacity of the laser fields begins by first finding the entropy lost by atoms, $\Delta S_a$. If the number of atoms is unchanged by the cooling process, the Sackur-Tetrode equation can be used to find $\Delta S_a = k_B \ln(V^{(\phi)}_{\rm final}/V^{(\phi)}_{\rm init})$ where $V^{(\phi)}$ is a phase-space volume. (For laser cooling, $\Delta S_a < 0$.) Moreover, the changes of the $V^{(\phi)}$'s are expressed by the product of the compression in velocity space $\Delta v_{\rm init}/\Delta v_{\rm final}$ with the expansion in configuration space $\Delta x_{\rm init}/\Delta x_{\rm final}$.

For the latter, we note that all laser cooling schemes have a characteristic cooling length and time found from the force and the velocity capture range $v_c$ of the force. The natural choice for the initial spatial extent of the atoms is this cooling length $\Delta x$. The largest distance atoms can travel during slowing is another $\Delta x$, and only a few atoms will reach $2\Delta x$. For calculational convenience, we choose the final spread to be $\Delta x_{\rm final} \approx \sqrt{2}\,\Delta x$ for each direction, a total of $2\sqrt{2}\,\Delta x$ in one dimension. For the width of the initial velocity distribution $\Delta v_{\rm init}$ we take the velocity capture range $v_c$ and for $\Delta v_{\rm final}$ we take some measure of the cooling limit. Thus $\Delta S_a = k_B \ln(2\sqrt{2}\,\Delta v_{\rm final}/v_c) < 0$, and is typically a few $\times\,(-k_B)$ per atom (it's surprising that $\Delta S_a$ is so small).

### 4. *Description of the Light Field*

It is straightforward to see how the light field absorbs entropy by calculating its density matrix $\rho_\ell$ before and after its interaction with atoms [26, 29]. This can be done in any basis, and we start with the light field in a pure state where $\rho_\ell = (\rho_\ell)^2$ so the entropy is zero. For the interaction with two-level atoms, we choose a basis of number states for the light beams as in the Jaynes-Cummings picture, and then properly entangle it with the ground and excited states of an atom, $|g\rangle$ and $|e\rangle$ respectively, to make a total wave function $\Psi$. The interaction with the atoms will change this to $\Psi'$. After evaluating the matrix $\rho'$ using the operator $|\Psi'\rangle\langle\Psi'|$ and then tracing over the two atomic states $|g\rangle$ and $|e\rangle$, it is clear that $\rho_\ell{}' \neq (\rho_\ell{}')^2$ [29, 30]. Thus the light field is no longer in a pure state so its entropy has increased to some positive value as a result of the interaction.

A sample of atoms immersed in a light field is neither a closed system nor is it in thermal contact with a reservoir, so the ordinary thermodynamic entropy cannot be defined. Instead we use the information definition $S = k_B \ln(N)$ where $N$ is the number of states accessible to the system. We find the entropy capacity of the light beams $\Delta S_\ell$ from $N$-values that are sufficiently distinct (small overlap) after the stimulated emission processes have redistributed the light energy among them.

Although the natural choice for a description of the laser beams might seem to be the familiar coherent states $|\alpha\rangle$, the strict definition of the $|\alpha\rangle$'s is not well-suited to the exchange of light between beams caused by absorption-stimulated emission cycles of atoms. In particular, the transition term of the Jaynes-Cummings Hamiltonian is $\propto (ab^\dagger + a^\dagger b)$, and although $|\alpha\rangle$ is an eigenstate of $a$, $a^\dagger|\alpha\rangle$ is a complicated object [31–33]. Moreover, the $|\alpha\rangle$'s are not eigenstates of the Hamiltonian $a^\dagger a$ nor are they orthogonal. Still, they represent a suitable approximation as long as it's recognized that absorption of light indeed *does* change the actual state of the field, even though in the exact (ideal) case, $|\alpha\rangle$ is an eigenstate of $a$ [31–34].

Even though the coherent states $|\alpha\rangle$ and $|\alpha'\rangle$ are not very good approximations, we may choose the "distinct state" criterion from the overlap formula $e^{-|\alpha-\alpha'|}$ to be $1/e$. Then this overlap condition requires distinct states to have $n$-values that differ by $\pm 2\sqrt{n}$, where $n \equiv |\alpha|^2$. Since Ref. [31] shows that the approximately coherent states are sub-Poissonnian, there are actually more accessible states than this lower limit estimate.

We need an estimate the field quantum number $n$, found from the amount of light that can interact with an atom in a large, cw laser beam. We choose a cylinder of base area equal to the on-resonance atomic absorption cross section $\sigma = 3\lambda^2/2\pi$ and of length $ct_{\rm cool}$, where $t_{\rm cool}$ is the the cooling time mentioned above. For a beam of intensity $I \equiv sI_{\rm sat}$ we find $n = I\sigma t_{\rm cool}/h\nu = s\gamma t_{\rm cool}/2$ where $I_{\rm sat} \equiv \pi hc\gamma/3\lambda^3$. ($\gamma$ appears as an artifact of the saturation intensity $I_s$ in $I$). For Doppler cooling, $n \sim 10^3$.

### 5. *Entropy Exchange*

The maximum change of $n$ required to stop an atom from $v = v_c$ is $\Delta n = Mv_c/\hbar k$ [35] and there are many different values of $\Delta n$ for the different atomic velocities in the sample, so many states of the light field can be populated. The number of independent states accessible to the laser field is $N = \Delta n/2\sqrt{n}$ so that

$$\Delta S_a + \Delta S_\ell = k_B \ln \underbrace{\left\{ \frac{2\Delta v_{\rm final}}{v_r} \frac{1}{\sqrt{s\gamma\, t_{\rm cool}}} \right\}}_{\equiv\ \eta} \tag{1}$$

where $v_r \equiv \hbar k/M$ is the recoil velocity. (Curiously, there is neither any dependence on $v_c$ in Eq. 1 nor buried in $\Delta v_{\rm final}$ or $t_{\rm cool}$.) Moreover, there is a one-to-one correspondence between the states of the light field and the atomic motional states [36] so their overlap is also small. As long as $\eta \sim 1$, meaning $\Delta S_\ell \sim |\Delta S_a|$, the light field has a large enough capacity to absorb the entropy lost by the atoms.

Further evaluation and discussion of Eq. 1 must be done case by case and the results are summarized in Table I [26]. The first two entries for Doppler molasses are readily calculated from the well-known Doppler limit and velocity damping constant [1, 37]. The cooling limit for Sisyphus cooling by polarization gradients, typically a few $\times\, v_r$ [1, 38], is taken from Eq. 4.37 of Ref. [39] ($\delta \equiv \omega_\ell - \omega_a$). The second entry is readily calculated from the increased velocity damping coefficient of Sisyphus cooling [39, 40].

The first entry for the bichromatic force, whose two frequencies are detuned by $\pm\,\delta$, comes from assuming that the atoms are finally distributed between two ground states (it could be more) [11], and the second entry comes from dividing the velocity cooling range by the (approximately constant) acceleration $2\hbar k\delta/\pi M$ [41]. The value $s = 3\delta^2/\gamma^2$ optimizes the bichromatic force (typically $\delta \sim 40\gamma$).

| | $\Delta v_{\rm final}/v_D$ | $\omega_r\, t_{\rm cool}$ | $\eta$ |
|---|---|---|---|
| Doppler molasses | 1 | 1 | $\dfrac{1}{\sqrt{s}}$ |
| Sisyphus cooling | $\sqrt{\dfrac{s\gamma}{2\delta}}$ | $\dfrac{\gamma}{\delta}$ | $\dfrac{1}{\sqrt{2}}$ |
| Bichromatic force | $\sqrt{\dfrac{\delta}{2\gamma}}$ | $\dfrac{\pi}{16}$ | $\sqrt{\approx 50\left(\dfrac{\gamma}{\delta}\right)}$ |

TABLE I: A summary of the values for entry into Eq. 1. The velocity limit of Doppler cooling is $v_D \equiv \sqrt{\hbar\gamma/(2M)}$. See text for a discussion. For Sisyphus cooling $\delta \equiv \omega_\ell - \omega_a$ is the laser detuning. For the bichromatic case, $2\delta$ is the frequency difference between the two fields, and typically $\delta \sim 40\gamma$.

Clearly $\eta \sim 1$ for all three cases so we can conclude that the laser beams themselves have sufficient capacity to absorb the entropy lost by the cooled atoms by redistribution of the laser light into a larger number of accessible states. Since the system is "open", the outgoing light beams carry away the entropy. Spontaneous emission is not required for this aspect of laser cooling. In some sense, this may be related to cavity cooling (see Ref. [42] and references therein).

We see that the entropy lost by the atoms can be transferred to the light field, and it's not dissipated until the outgoing light hits the walls. Since the walls are NOT part of the system, this final destruction of the light field is indeed a dissipative, non-conservative, and irreversible process. The walls are not part of the system, just as the empty modes into which spontaneous emission dumps the light are not part of the system in the common $(\Delta E, \Delta p)$ pictures of Doppler cooling. The model here is different from those of previously studied cases [28, 43, 44] because the applied light field is a dynamical variable of the Hamiltonian.

### 6. *The Role of Spontaneous Emission in Laser Cooling*

Although it's now clear that spontaneous emission is not required to carry away the entropy removed from a vapor atoms during laser cooling, it is also true that spontaneous emission is indeed crucial for energy exchange in some forms of laser cooling. Since excited atoms don't absorb resonantly, their return to the ground state without the spontaneous emission needed for further absorption can only occur by stimulated emission. If it occurs by the original exciting beam, there is no net energy exchange in the process. If stimulated emission is induced by another beam, for example the counterpropagating beam in Doppler molasses or Sisyphus cooling, then the absorption-stimulation emission sequence in the opposite order is equally likely when spatially averaged over a wavelength, and on average there is no net energy transfer.

For Doppler molasses, only spontaneous emission between absorptions can exploit the Doppler shifts to allow energy loss because the average frequency of the emitted light is $\omega_a > \omega_\ell$. For Sisyphus cooling, spontaneous emission is needed for the transitions between the top of one potential hill of the light shift to the bottom of another [39]. Without it, the energy exchange is limited to the light shift, and that is usually much smaller than atomic kinetic energies. Thus the indispensable role of spontaneous emission in many forms of laser cooling is not for entropy dissipation, but for energy transfer.

By contrast, the bichromatic force (BF) has no such limits [2, 11]. With appropriate parameters and spatial offsets of the standing waves of the two different frequencies, there are positions where the light shifts and detuning just cancel, and exact crossings of the eigenstates can occur. Atoms can mediate the exchange of red-detuned light for blue, and vice versa, resulting in energy exchange between the atoms and the light

beams [11]. Thus energy conservation and entropy dissipation for the BF are accomplished differently so that spontaneous emission is not necessary for any of them. This mechanism has no significant limit on the energy scale of interest here, and more important, has no counterpart in monochromatic light [26].

The BF is indeed velocity dependent, but it's not at all like the more familiar friction forces of other laser cooling schemes. Here the non-adiabatic transitions provide the origin of the velocity dependence of the force, and depend exponentially on the velocity [11]. There is no traditional friction or damping force. Thus the BF is different from other laser cooling schemes because spontaneous emission is NOT needed to mediate the energy exchange nor to produce a velocity-dependent force.

We have seen how the light beams have the capacity to absorb the entropy lost by laser cooled atoms, and that spontaneous emission is not required for this task. We have also seen that it is indeed required to mediate the energy loss of the atoms in some forms of laser cooling. The combination of these two results provides a completely different view of the role of spontaneous emission in laser cooling.

### C. Nanofabrication with He* Using Bichromatic Beam Collimation

#### *1. Introduction*

Atomic nano-fabrication (ANF) has many special features that distinguish it from other methods [19] and these were outlined in the proposal for the expired grant. At that time we proposed to do ANF with metastable $2^3S$ helium (He*) very efficiently because we could use the bichromatic force to get a high He* intensity so that the exposure time could be very short. Here we report success in doing precisely this.

The ability to record and preserve the positions of atoms in a permanent structure on a sub-micron scale has myriad possible applications. To begin, the structure itself may be of value. Such nano-scale patterns can be made with precise long-range regularity whose spacing is known to spectroscopic precision. Examples include gratings for short wavelength radiation, photonic crystals, metamaterial samples, and many others. Second, the distribution of atoms is determined by light fields so that the pattern produced can be used as a measure of the light intensity distribution. For example, very small deviations caused by wave front imperfections could be detected. Finally, the process by which the light fields influence the atomic motion in forming such patterns is an interesting topic of study by itself.

Atom lithography with a positive resist works by destroying the chemical bonds in a layer of polymeric molecules of self-assembled monolayers (SAM's), then dissolving the damaged molecules, and finally etching the exposed area (see Fig. 6). Using the metastable $2^3S$ state of helium (He*) is ideal for this because its internal energy of 20 eV is higher than any other metastable atom. Thus it is most effective for exposing a resist with minimum dosage and therefore shortest exposure time and thus minimum restrictions on the atomic beams and laser control [19].

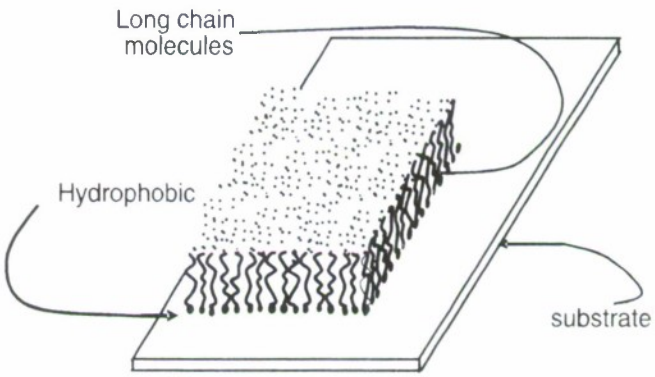


FIG. 6: The drawing shows an artistic rendition of a fabricated SAM on a substrate. The long chain molecules orient themselves with their hydrophobic heads bound to the substrate and their long-chain hydrophillic tails sticking out into the solution. The result resembles an ordinary carpet pile as shown. Incident He* atoms release their 20 eV internal energy somewhere along the chain and therefore weaken or actually break the bond that holds it together. Then an acid solution dissolves away the alcanethioles and leaving the substrate exposed for further etching.

In our first experiments, we planned to pattern a resist on a SAM over gold using a physical mask (just a screen) with our bright He* beam. We found excellent results with a beam that was collimated with the bichromatic force followed by two transverse Doppler molasses stages for further cooling. The metal screen projected its image on a SAM of nonanethiol and the undisturbed SAM regions then protected a gold coated silicon wafer from a wet chemical etch. The open areas of the screen allowed incident He* to damage the SAM molecules by depositing their 20 eV of internal energy on the surface. Samples created with this method had an edge resolution of about 60 nm that was measured with an atomic force microscope.

Then we succeeded with nanolithography using a standing wave to make the patterns. Moreover, the parameters of this optical standing wave extended into a previous unexplored range. In particular, there are two domains of laser intensity used for steering the atoms into the desired patterns. Our experiments are in the lower intensity region called the focusing regime (at higher intensities it's called the channelling regime). Although our numerical simulations of atomic focussing by a laser standing wave suggest that we cannot produce patterns in this regime when the atomic beam has a relatively large angular divergence, we have collimated our beam sufficiently to accomplish such patterning at such lower intensities. Smaller features can be obtained in the focussing regime than in the channelling regime [20].

### 2. *Numerical Calculations*

In preparation for our experiments, we did numerical calculations to determine the neighborhood of our operating parameters. The first of these were simple trajectories of atoms incident perpendicular to a standing wave with transverse Gaussian intensity distribution. We found trajectories corresponding to both the focusing and channelling regimes, and especially had a close look at the region between them.

Since our choice of a perfectly collimated, mono-velocity beam incident exactly at $\pi/2$ is unrealistic, we also performed a Monte-Carlo simulation of the paths and landing points of the atoms. The single longitudinal and transverse velocities were replaced by distributions characterized by widths that are correlated. The simulation results showed the formation of half-wavelength size structures over a wide range of parameters. The pure focusing regime for the parameters reflecting our experimental setup was not found to produce patterning; but the simulations indicated that pattern formation was more sensitive to atomic beam divergence as opposed to atomic beam chromaticity. In both the trajectory and Monte-Carlo calculations, our results differed very little from those previously published in Ref's [21, 22].

### 3. *Experiment*

We achieved neutral atom lithography using a bright beam of He* that originates from a reverse flow DC discharge source [23, 24]. It has a slightly supersonic longitudinal velocity distribution centered near 1100 m/s and is about ± 200 m/s wide. This atomic beam is collimated with the bichromatic force [12], followed by three optical molasses velocity compression stages [25]. Because bichromatic collimation makes such an intense He* beam, our exposure time is measured in minutes instead of hours. We have observed the focusing and channeling of the He* beam by the dipole force the atoms experience while traversing a standing wave of $\lambda = 1083$ nm light tuned 490 MHz above the $2^3S_1 \rightarrow 2^3P_2$ transition.

In our experiment the bichromatic force is implemented with counter-propagating light beams, each containing two frequencies that are separated by $2\delta = 2\pi \times 120$ MHz. All the light originates from diode lasers stabilized by saturated absorption spectroscopy, frequency shifted by various AOM's, and amplified by Yb-doped fiber amplifiers. The laser linewidths, both before and after the fiber amplifiers, are measured by heterodyne spectroscopy to be less than 0.25 MHz.

If frequencies of these beams were centered about the atomic resonance, the dependence of the force on atomic velocity $v$ would be symmetric about $v = 0$ over the velocity range $\pm\delta/2k$ and nearly vanish elsewhere [2]. Since collimation requires the force to be antisymmetric about $v = 0$, we shift the velocity dependence by $\delta/2k$ without changing its shape by shifting the laser frequencies appropriately [12]. The resulting force is unidirectional so there are two collimation regions for each of two dimensions, making four bichromatic force regions. The four sequential bichromatic force regions are placed as close as possible to the cone of He* atoms emerging from the source so that the collimated beam has a minimum diameter [25]. Each region is 11 mm long, and their apodized Gaussian beam profiles carry an average intensity of 4000 $I_s$, where the saturation intensity $I_s \equiv \pi hc/3\lambda^3\tau \approx 0.16$ mW/cm$^2$.

The transverse velocity spread of the atoms in the beam after the bichromatic force regions is well above ±10 m/s corresponding to $\sim \pm 9$ mrad, and is not suitable for our purposes. Therefore we have a "booster" molasses stage with detuning many times larger than the natural width $\gamma$ to capture atoms in this large angular spread, followed by an ordinary Doppler molasses to bring the atomic beam divergence down to nearly 1 mrad with very little loss of atoms (the Doppler limit is $\sim 0.25$ mrad). This collimation occupies 8.2 cm of our beamline and delivers $\sim 1.5 \times 10^9$ atoms/s-mm$^2$ at our sample, 68 cm from the He* source [25].

Our beam of He* atoms is focussed into lines by a standing wave field of $\lambda = 1083$ nm light tuned $\sim$ 490 MHz above atomic resonance (atoms attracted toward the nodes). It has an elliptical cross section with waist of $\sim 1.5$ mm parallel to the substrate surface and of $\sim 330\,\mu$m along the atomic beam path and a peak

intensity of 1.48 W/cm$^2$. The intensity of this standing wave can be varied from the intensity of the focusing regime to over 37 W/cm$^2$, well into the channelling regime [22].

Our samples are built on single-crystal silicon wafers that have a 200 Å layer of gold evaporated onto their [100] surface over a 5 Å chromium adhesion layer. These wafers are grown and coated commercially. The SAM is assembled onto the gold surface by submersing the wafer in a 1 mM solution of nonanethiol in ethanol for 13 to 20 hours. The long chain molecules orient themselves with their hydrophobic heads bound to the gold substrate and their long-chain hydrophillic tails sticking out into the solution as in Fig. 6.

The incident He* attacks the structure of the SAM molecules thereby making it soluble in a wet chemical etch where the undisturbed SAM protects parts of the gold layer and the unprotected gold regions are dissolved. Thus a 10 minute exposure deposits one He* in each $\sim 100\,\text{Å}^2$ area without any focussing, and the focussing could easily increase this dosage to a few He* per SAM molecule site (area $\sim 30\,\text{Å}^2$, estimated). Samples created with this method have an edge resolution of $\sim 80$ nm that we measured with an atomic force microscope. This seems to be limited by the domain granularity of the gold layer and the etching process. This method of neutral atom lithography is analogous to ordinary resist-based technologies that are used in most conventional lithography processes.

Figure 7 shows $\sim 200$ lines spanning about $100 \times 65\,\mu$m of a $3 \times 3$ mm region (less than 1/1000 of the total area) that was quite uniformly patterned. The unfocused dosage of He* was $3 \times 10^{12}$atoms/mm$^2$ during the 36 minute exposure. The intensity of the light mask beam used for patterning was 5.93 W/cm$^2$, about four times $I_s$ and corresponding to $\sim 4$ times the 1.48 W/cm$^2$ threshold for the focusing regime. It is cut in the middle by the substrate, as on the left side of Fig. 3 in Ref. [19]. Thus its width is 3 mm along the surface perpendicular to its $\vec{k}$-vectors (twice the waist) and the atoms travel $\sim 330\,\mu$m through half of it before hitting the SAM-coated substrate.

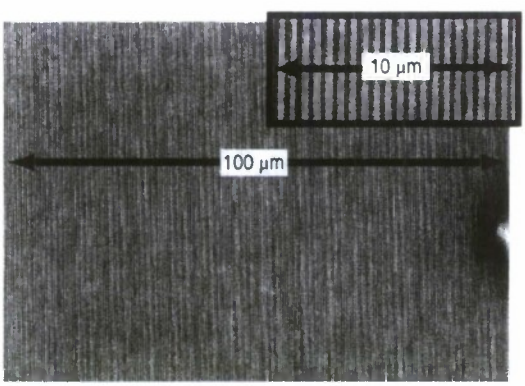


FIG. 7: Scanning electron microscope image of one sample. There are $\sim 200$ vertical lines on this figure separated by 541.3 nm $= \lambda/2$. The unfocused peak dosage was $3 \times 10^{12}$ atoms/mm$^2$ during the 31 minute exposure. The inset is a small portion magnified by 5 since aliasing of the image in print or on screen may cause deception even though its texture has been smoothed for reproduction.

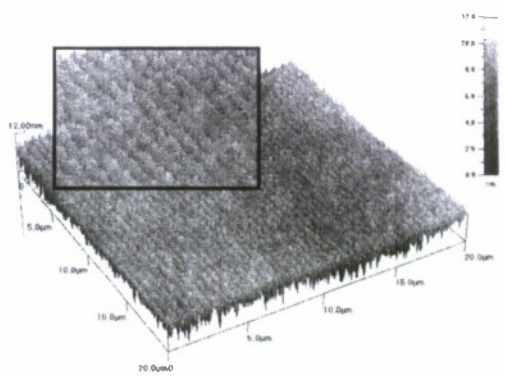

FIG. 8: Atomic force microscope image of the same wafer as Fig. 7. This image has a 5 pt smoothing but still clearly shows both the graininess of the original gold coating and the resolution of the AFM.

Figure 8 shows the AFM image of the same sample. The angular view shows that the depth of the lines is nearly the full 10 nm thickness of the gold layer and that the spatial resolution is limited by its graininess to about 1/5 of the line separation, 100 nm.

Our fabrications have been reliable and repeatable, sample after sample, over a period of months. In a standing wave arranged to focus the He* into lines separated by $\lambda/2$ on the sample, our lines cover the entire exposed length of the substrate, about 3 mm. They are 3 mm long, corresponding to about twice the beam waist of the laser standing wave. Thus there are $\sim 6 \times 10^3$ lines of length $\sim 2800\,\lambda$ as shown in Fig. 7 [25].

### D. Student Progress and Other Contributions of Naval Interest

Since our institution is a university, our primary outcome of special interest to the Navy is educational. Our program cannot possibly compete with major institutions devoted to time-keeping and navigation, but we **DO** provide the educated scientists necessary for their operation. For example, current graduate student Matthew Eardley is pursuing his Ph.D. thesis research in the Chip Scale Atomic Devices group at N.I.S.T. in Boulder, CO. The group is developing gyroscopes, magnetometers, and clocks that all take advantage of MEMS technology to produce low-cost, low-power, portable microchip-scale devices that derive high stability and accuracy from the energy levels of laser-pumped atoms in microfabricated vapor cells. Although this kind of work cannot be supported in our laboratory, the education and training he received here is vital to his thesis research there.

As another example, 2002 Ph.D. Matt Cashen did a post-doc with Mark Kasevich at Stanford University on precision gravimetry, certainly important for submarine detection. Then he started a permanent job in the Lasers Division of Raytheon Corp. working on atomic clocks. The results of his research has been passed off to Symmetricom for further development. Matt has used his background to advance the state of the art in sensors for precision inertial navigation systems such as accelerometers and gyroscopes. All such devices are based on ultra-cold atomic techniques and have the potential to revolutionize military navigation systems. Scientists with his kind of training in laser cooling and trapping techniques are vital to the development of next generation sensors for military applications. This shows the value of training Ph.D. scientists who will enable the transition of this technology from the lab into the field.

There are other facets of our educational activities, and part of its graduate component is summarized in the chart below. In the past three years we will have finished four Ph.D.'s, three of whom have already taken jobs in physics. The six visiting M.A. students from our exchange programs (five from Würzburg) have all returned home and begun Ph.D. studies at various universities. Some of our undergraduates have won prestigious awards, and all of them are in Ph.D. programs at excellent universities. Our Laser Teaching Center students are not listed in this chart.

| Year | Ph.D. | M.A. | Undergraduate |
|---|---|---|---|
| 2004 | Matt Partlow<br>*post-doc at U. Toronto* | Jörg Böchmann<br>*Univ. of Würzburg, now at München* | Melissa Friedman[1]<br>*now grad at Oxford* |
| 2005 | | Matthias Riedmann<br>*Univ. of Würzburg, now at Hannover* | Kyung Choi<br>*Stony Brook undergrad* |
| 2006 | Seung-Hyun Lee<br>*now at Korean Military Institute*<br>Xiyue Miao<br>*postdoc at Stony Brook* | Esther Wertz<br>*returned to Univ. Paris VII*<br>Mike Keller<br>*Univ. of Würzburg, now at Vienna*<br>Andy Vernaleken<br>*Univ. of Würzburg, now at München* | Maaneli Derekhshani<br>*Stony Brook undergrad*<br>Kyung Choi<br>*now grad at Caltech*<br>Tak Chu Li<br>*now grad at U. MD.* |
| 2007 | | Benedikt Scharfenberger<br>*Univ. of Würzburg, now at Siegen* | Thien An Nguyen<br>*Stony Brook undergrad* |

[1] Won prestigious Marshall Fellowship and now in graduate school at Oxford University.

[1] H. Metcalf and P. van der Straten, *Laser Cooling and Trapping* (Springer, New York, 1999).
[2] J. Söding, R. Grimm, Y. Ovchinnikov, P. Bouyer, and C. Salomon, Phys. Rev. Lett. **78**, 1420 (1997).
[3] T. Lu, X. Miao, and H. Metcalf, Phys. Rev. A **71**, R061405 (2005).
[4] T. Lu, X. Miao, and H. Metcalf, Phys. Rev. A **75**, 063422 (2007).
[5] X. Miao, E. Wertz, M. G. Cohen, and H. Metcalf, Phys. Rev. A **75**, 011402 (2007).
[6] X. Miao, B. Scharfenberger, M. G. Cohen, and H. Metcalf (????), in preparation.
[7] M. Williams, F. Chi, M. Cashen, and H. Metcalf, Phys. Rev. A **60**, R1763 (1999).
[8] M. Williams, F. Chi, M. Cashen, and H. Metcalf, Phys. Rev. A **61**, 023408 (2000).
[9] M. Cashen and H. Metcalf, Phys. Rev. A **63**, 025406 (2001).
[10] M. Cashen, O. Rivoire, V. Romanenko, L. Yatsenko, and H. Metcalf, Phys. Rev. A **64**, 063411 (2001).
[11] L. Yatsenko and H. Metcalf, Phys. Rev. A **70**, 063402 (2004).
[12] M. Partlow, X. Miao, J. Bochmann, M. Cashen, and H. Metcalf, Phys. Rev. Lett. **93**, 213004 (2004).
[13] M. Cashen, O. Rivoire, L. Yatsenko, and H. Metcalf, J. Opt. B: Quant. Semiclass. **4**, 75 (2002).
[14] M. Cashen and H. Metcalf, J. Opt. Soc. Am. B **20**, 915 (2003).
[15] X. Miao, Ph.D. thesis, Stony Brook University (2006).
[16] L. P. Yatsenko, S. Guérin, and H. R. Jauslin, Phys. Rev. A **65**, 043407 (2002).
[17] D. Sawicki and J. H. Eberly, Optics Express **4**, 217 (1999).
[18] Paul Berman, private communication.
[19] D. Meschede and H. Metcalf, J. Phys. D: Appl. Phys. **36**, R17 (2003).
[20] W. R. Anderson, C. C. Bradley, J. J. McClelland, and R. J. Celotta, Phys. Rev. A **59**, 2476 (1999).
[21] J. J. McClelland, R. E. Scholten, E. C. Palm, and R. Celotta, Science **262**, 877 (1993).
[22] J. J. McClelland, J. Opt. Soc. Am. B **12**, 1761 (1995).
[23] J. Kawanaka, M. Hagiuda, K. Shimizu, F. Shimizu, and H. Takuma, Appl. Phys. B. **56**, 21 (1993).
[24] H. Mastwijk, M. van Rijnbach, J. Thomsen, P. van der Straten, and A. Niehaus, Eur. Phys. J. D **4**, 131 (1998).
[25] C. Allred, Ph.D. thesis, Stony Brook University (2009).
[26] H. Metcalf, Phys. Rev. A **77**, R 061401 (2008).
[27] W. E. Lamb, App. Phys. B **60**, 77 (1995).
[28] W. Ketterle and D. E. Pritchard, Phys. Rev. A **46**, 4051 (1992).
[29] E. Boukobza and D. J. Tannor, Phys. Rev. A **71**, 063821 (2005).
[30] D. Tannor and A. Bartana, Journal of Physical Chemistry A **103**, 10359 (1999).
[31] G. S. Agarwal and K. Tara, Phys. Rev. A **43**, 492 (1991).
[32] A. Zavatta, S. Viciani, and M. Bellini, Science **306**, 660 (2004).
[33] V. Parigi, A. Zavatta, M. Kim, and M. Bellini, Science **317**, 1890 (2007).
[34] B. R. Mollow, Phys. Rev. A **12**, 1919 (1975).
[35] The momentum change for an absorption-stimulated emission cycle between counterpropagating beams is $2\hbar k$, but two beams are affected so the factors of 2 cancel.
[36] S. J. van Enk and H. J. Kimble, QIC **2**, 1 (2002), URL `http://www.citebase.org/abstract?id=oai:arXiv.org:quant-ph/0107088`.
[37] D. Wineland and W. Itano, Phys. Rev. A **20**, 1521 (1979).
[38] C. Salomon, J. Dalibard, W. Phillips, A. Clairon, and S. Guellati, Europhys. Lett. **12**, 683 (1990).
[39] J. Dalibard and C. Cohen-Tannoudji, J. Opt. Soc. Am. B **6**, 2023 (1989).
[40] Caution is needed since Eq. 4.3 of Ref. [39] defines the Rabi frequency to be twice as large as that used here. Our definition is $\hbar\Omega \equiv \vec{d} \cdot \vec{\mathcal{E}}$.
[41] In Ref's. [9, 12] the velocity range was measured to be $\delta/k\,(\pm\delta/2k)$ but in Ref. [11] it was shown that the part of the bichromatic force that arises from the mechanism described therein has a range $\delta/2k\,(\pm\delta/4k)$.
[42] K. Mürr, Phys. Rev. Lett. **96**, 253001 (2006).
[43] M. E. Carrera-Patio and R. S. Berry, Phys. Rev. A **34**, 4728 (1986).
[44] S. van Enk and G. Nienhuis, Phys. Rev. A **46**, 1438 (1992).